Accepted Manuscript

Supramolecular polymeric chemotherapy based on cucurbit[7]uril-PEG copolymer

Hao Chen, Yueyue Chen, Han Wu, Jiang-Fei Xu, Zhiwei Sun, Xi Zhang

PII: S0142-9612(18)30151-0

DOI: 10.1016/j.biomaterials.2018.02.051

Reference: JBMT 18524

To appear in: *Biomaterials*

Received Date: 30 December 2017

Revised Date: 8 February 2018

Accepted Date: 27 February 2018

Please cite this article as: Chen H, Chen Y, Wu H, Xu J-F, Sun Z, Zhang X, Supramolecular polymeric chemotherapy based on cucurbit[7]uril-PEG copolymer, *Biomaterials* (2018), doi: 10.1016/j.biomaterials.2018.02.051.

Supramolecular polymeric chemotherapy based on cucurbit[7]uril-PEG copolymer

Hao Chen [a, 1], Yueyue Chen [b, 1], Han Wu [a], Jiang-Fei Xu [a], Zhiwei Sun [b, *], Xi Zhang [a, **]

[a] *Key Lab of Organic Optoelectronics & Molecular Engineering, Department of Chemistry, Tsinghua University, Beijing 100084, China.*

[b] *Department of Toxicology and Sanitary Chemistry, School of Public Health, and Beijing Key Laboratory of Environmental Toxicology, Capital Medical University, Beijing 100069, China*

* Corresponding author.

** Corresponding author.

Email addresses: zwsun@ccmu.edu.cn (Z. Sun), xi@mail.tsinghua.edu.cn (X. Zhang).

[1] Hao Chen and Yueyue Chen contributed equally to this work.

Abstract

We develop a strategy of supramolecular polymeric chemotherapy based on a new kind of water-soluble polymer that bears cucurbit[7]uril (CB[7]) in the main-chain. To this end, we synthesized a bis-alkynyl functionalized CB[7] and polymerized it with α,ω-diazide-PEG through click reaction to form the desired CB[7] based main-chain polymer (poly-CB[7]). Anticancer drug, oxaliplatin, could be encapsulated into the cavity of poly-CB[7] to form a supramolecular polymeric complex, which displayed low cytotoxicity to normal cells. In addition, the cytotoxicity of the oxaliplatin was recovered when the complex met cancer cells that could overexpress spermine, e.g. colorectal cancer cell, through competitive replacement of oxaliplatin from CB[7] cavity by spermine. Interestingly, the cytotoxicity of the supramolecular polymeric complex to cancer cells is higher than oxaliplatin itself. The enhanced cytotoxicity should result from a combined effect by combining the release of

oxaliplatin from the supramolecular polymeric complex and decrease of spermine in the micro-environment of the cancer cells, as spermine is needed for cell growth and proliferation. One more advantage of the supramolecular polymeric complex is its long circulation performance *in vivo* compared with the supramolecular complex between oxaliplatin and CB[7]. Therefore, this line of research may open new horizons for supramolecular polymeric chemotherapy.

Keywords:

supramolecular materials

cucurbituril

polymeric therapeutics

supramolecular chemotherapy

oxaliplatin

1. Introduction

Chemotherapy is among one of the most important clinical ways for cancer treatment [1]. Many kinds of chemical drugs have been developed for chemotherapy, such as paclitaxel [2,3], camptothecin [4,5], doxorubicin [6], and platinum-based drugs [7,8]. Although it has gained significant clinic success, these drugs also face problems including limited selectivity, bioavailability, poor solubility and severe side-effects [9]. To address on the problems, a lot of drug delivery systems including micelles, liposomes and nano-carriers have been developed, which are greatly helpful in dealing with those problems [10-24]. To date, some of such drug delivery systems have been approved, such as Doxil [25], Abraxane [26] and Genexol-PM [27].

In addition to non-specific interaction, specific non-covalent interactions with stronger binding affinity including host-guest interaction were considered for drug delivery with promising capability such as enhanced drug stability and decreased toxicity [28-30]. In our previous work, we have introduced a new concept of supramolecular chemotherapy, which is aimed to employ supramolecular approach for not only decreasing the cytotoxicity of clinical

anticancer drugs to normal cells but also improving their cytotoxicity to cancer cells [31-33]. In detail, the cytotoxicity of anticancer drugs can be decreased through the encapsulation of the drugs in host molecules, such as cucurbit[7]uril (CB[7]) and carboxylated pillar[6]arene. The anticancer drugs can also be selectively released for killing cancer cells through competitive replacement of overexpressed tumor biomarker, spermine [34,35]. Through the combined effect of the recovery of cytotoxicity of drugs through competitive replacement of drugs by spermine and the consumption of spermine, the cytotoxicity of anticancer drugs to cancer cells is enhanced [28-30]. This supramolecular chemotherapy strategy works well with cancer cells which can overexpress spermine, such as colorectal and lung cancer cells. Although supramolecular chemotherapy has its advantage of low cytotoxicity to normal cells and high cytotoxicity to cancer cells, other performance of therapeutic agents, for example circulation performance, need to be improved.

Inspired by the concept of polymer therapeutics raised by Ringsdorf [36-38], we attempted to combine the advantage of supramolecular chemotherapy and polymer therapeutics through marrying supramolecular recognition units with polymeric structures, and therefore develop a new strategy of supramolecular polymeric chemotherapy. PEGylation is a widely accepted method to enhance the bioavailability of drugs [39,40]. Through PEGylation, the apparent molecular weight of drugs increases, which results in the decrease of kidney excretion of the drugs. Moreover, the strong hydrophilicity of PEG chains helps the drug avoid fast recognition by the immune systems and reduces clearance of drugs from the body. Hence we assume that such a combination would be helpful in maintaining the advantage of supramolecular chemotherapy as well as improving circulation performance of the anticancer drugs.

As shown in Scheme 1, we designed a main-chain polymer, poly-CB[7], that bear CB[7] and PEG motifs, and employed the polymer as drug carrier for supramolecular polymeric chemotherapy. CB[7] is recognition site for drug and biomarker which is essential for supramolecular chemotherapy [31,32]. PEG chain endows the polymer with long circulation ability and good solubility [39,40]. As a proof of concept, oxaliplatin, a clinical anticancer drug [7], was encapsulated into the cavity of CB[7] in poly-CB[7], and the cytotoxicity of oxaliplatin to normal cells could be significantly decreased in this way. When poly-CB[7]

bearing oxaliplatin met cancer cells which can overexpress spermine, such as colorectal cancer cells [34,35], oxaliplatin could be released from poly-CB[7] by competitive replacement of spermine, leading to recovery of the cytotoxicity of oxaliplatin. Combining the supramolecular chemotherapy with PEGylation, it is anticipated that decreased cytotoxicity to normal cells, increased cytotoxicity to cancer cells and enhanced circulation performance *in vivo* of the oxaliplatin would be realized simultaneously, opening a new horizon for supramolecular polymeric chemotherapy.

2. Materials and methods

2.1. Materials

Propargyl bromide, ammonium persulphate and α,ω-diazide polyethylene glycol (M_n = 2000) were purchased from J&K Scientific. Spermine was obtained from TCI. Oxaliplatin was purchased from Meilunbio. CHP 20P resin was obtained for Mitsubishi Chemical. All of the chemicals were used as received without further purification. Cucurbit[7]uril (CB[7]) [41,42], tris[1-(3-hyroxypropyl)-1*H*-1,2,3-triazol-4-yl]methanol·CuCl (THPTM·CuCl) [43] and 3,3'-(Octane-1,8-diyl)-*bis*-(1-ethyl-imidazolium) bromide (C_8bim) [44] were synthesized according to the procedures in literatures.

2.2. General characterizations

NMR spectra were recorded on a JOEL ECS-400 spectrometer in deuterium oxide at 298 K. For ^{1}H NMR, the solvent peak of HOD at 4.79 ppm was used as the internal standard. HR-MS was measured on a Thermo LTQ mass spectrometer. Isothermal titration calorimetry (ITC) experiments were performed on a Microcal VP-ITC apparatus at 298 K. Molecular weight of poly-CB[7] was tested through gel permeation chromatography coupled with multi-angle laser scattering (GPC-MALLS). In detail, the experiment was performed on an Agilent 1260 infinity liquid chromatography system coupled with Wyatt multi-angle light scattering detector (DAWN HELEOS-II) and differential refraction detector (Optilab rEX), with 50 mM $NaNO_3$ aqueous solution as eluent. UV-vis spectra were recorded on a HITACHI U-3010 spectrometer. For competitive replacement of oxaliplatin from poly-CB[7] by spermine, 100 mM spermine was employed to titrate 0.2 mM oxaliplatin/poly-CB[7] complex. The content of platinum in samples was tested on a Perkin Eimer SCIEX ELAN DRC-e ICP

mass spectrometer.

2.3. Sample synthesis

General procedures for the synthesis of poly-CB[7] are shown in Scheme 2.

2.3.1. Synthesis of bis-hydroxyl-CB[7] [CB[7](OH)$_2$]

The synthesis procedure of CB[7](OH)$_2$ was modified from a reported procedure of CB[7]OH [45]. In detail, CB[7] (5.0 g, 4.3 mmol) and C_8bim (2.0 g, 4.3 mmol) were dissolved in 300 mL deionized water. The solution was degassed with nitrogen and heated to 70 ˚C. Then $(NH_4)_2S_2O_8$ (2.28 g, 10 mmol) was added and the solution was heated to 85 ˚C for 5 h. Afterward, the solution was concentrated to 30 mL, and CB[7](OH)$_2$ was isolated through liquid chromatography with column packed with CHP-20P macroporous resin. The compositions of eluent were monitored by employing HR-MS. CB[7] was eluted first, followed by CB[7]OH, and finally CB[7](OH)$_2$. The CB[7](OH)$_2$ fractions were collected and concentrated until the solution looked viscous. Then CB[7](OH)$_2$ was precipitated with methanol as white solid in the form of host-guest complex with C_8bim (1.2 g, yield is 17%). Detailed characterization of CB[7](OH)$_2$ is available in supplementary data.

2.3.2. Synthesis of bis-alkynyl-CB[7] [CB[7](OA)$_2$]

The synthesis procedure of CB[7](OA)$_2$ was modified from a reported procedure of CB[7]OA [46]. In detail, CB[7](OH)$_2$·C_8bim (1.2 g, 0.74 mmol) was dispersed in 10 mL anhydrous DMF, then 40 mL anhydrous DMSO was slowly added and the solid was suspended under stirring. NaH (0.32 g, 8.0 mmol, 60% in mineral oil) was added, and the suspension was stirred for 2 h under nitrogen atmosphere. Then the suspension was cooled down to 0 ˚C, and propargyl bromide (1.8 g, 12 mmol, 80% toluene solution) was added. The temperature of the solution was slowly recovered to room temperature and the reaction was performed for 6 h. Afterward, the solution was precipitated with methanol, and the precipitate was washed with methanol twice and dried under vacuum to obtain raw CB[7](OA)$_2$ as gray solid (1.1 g). Detailed characterization of CB[7](OA)$_2$ is available in supplementary data.

2.3.3. Synthesis of poly-CB[7]

Raw CB[7](OA)$_2$ (1.0 g) was dissolved in 10 mL H_2O with the support of 0.4 g C_8bim. Insoluble fraction was removed through centrifugation. Then α,ω-diazide PEG was added gradually. The ratio of CB[7](OA)$_2$ and α,ω-diazide PEG was monitored by employing ^{1}H

NMR to guarantee 1:1 molar ratio of the two monomers. Then THPTM·CuCl (5.0 mg, 0.01 mmol) was added as catalyst, and the reaction was performed at 55 ˚C under nitrogen atmosphere for 24 h. The polymer solution was firstly dialyzed against deionized water for 24 h to remove excess C_8bim and other soluble impurities. Then the polymer solution was dialyzed against 1 g/L CB[7] solution for 24 h to remove the complexed C_8bim in the CB[7] cavity of poly-CB[7], and this process was repeated for 3 times. Finally, the polymer solution was dialyzed against deionized water again for 36 h to obtain poly-CB[7]. The concentration of the solution was determined through internal standard method with trimethyl adamantyl ammonium iodide by using ^{1}H NMR. Detailed characterization of poly-CB[7] is available in supplementary data.

2.4. Cell culture and cytotoxicity determination

The colorectal cancer cell line HCT116 and the colorectal normal cell line NCM460 were purchased from American Type Culture Collection (ATCC, Rockeville, MD). The cells were cultured in Roswell Park Memorial Institute 1640 (RPMI1640) containing 10% fetal bovine serum, 1% penicillin-streptomycin (penicillin 100 U/mL and streptomycin 100 μg/mL) in a humidified incubator at 37 °C with 5% CO_2 humidified atmosphere. In viability assays, the cells were seeded in 96-well plates at 3000 cells per well until the cells reached 60−70% confluency. Then the corresponding drugs were added and the cells were kept incubating for 24 h. After incubation, the cells were washed with culture media, and cell proliferation was measured using the cell counting kit-8 (CCK-8, Dojindo Laboratories Kumamoto, Japan). Absorbance of the bio-reduced soluble formazan product was measured at 450 nm using a Versamax microplate reader. Results were quantified by manually subtracting the blank value from each value then normalizing against the control values.

2.5. Animal experiments

Male BALB/c nude mice and male KM mice (4-6 weeks old) were purchased from and taken care by Beijing Vital River Laboratory Animal Technology Co., Ltd. (Beijing, China). The mice were kept under specific pathogen-free conditions with standard and sterilized water and food. And they received care in compliance with the guidelines outlined in the Guide for the Care and Use of Laboratory Animals.

2.6. Plasma clearance of oxaliplatin

Seventy-two male KM mice (6 weeks old) were randomly divided into three groups including oxaliplatin/poly-CB[7] group, oxaliplatin/CB[7] group and oxaliplatin group. Each group contained 24 mice. The corresponding drugs were intravenously injected with dose of 5 mg oxaliplatin per kg of mouse body weight. Blood samples were collected at predetermined time points (0.25, 0.5, 1, 2, 4, 8, 12 and 24 h) from the retro-orbital plexus of the mouse eye. The blood samples were then placed in heparinized tubes and centrifuged to obtain plasma. The plasma samples were digested with HNO_3 and $HClO_4$, and the content of platinum was determined by employing ICP-MS.

2.7. Tumor xenograft models

The HCT116 xenograft tumor models were generated by hypodermic injection of 1×10^6 cells (0.2 mL suspension) in BALB/c nude mice (4 week old). The tumor volume was calculated with (tumor length) × (tumor width)^2/2. The tumor volumes reached around 100 mm^3 after 13 days of post-tumor inoculation, which was ready for tumor inhibition study.

2.8. Tumor inhibition study

Forty HCT116 xenograft mice was divided into four groups including control group, oxaliplatin/poly-CB[7] group, oxaliplatin/CB[7] group and oxaliplatin group. Each group contained 10 mice. The corresponding drugs were intravenously injected with dose of 5 mg oxaliplatin per kg of mouse body weight. The mice received injection for six times on Monday, Wednesday and Friday during two weeks. During these days, the tumor volume and body weight of all mice were also monitored.

2.9. Tissue distribution study

Tissue distribution study of platinum is composed of two parts. To characterize the distribution in heart, liver, spleen, lung and kidney, twelve male KM mice (6 weeks old) were randomly divided into three groups including oxaliplatin/poly-CB[7] group, oxaliplatin/CB[7] group and oxaliplatin group, respectively. Each group contained 4 mice. The corresponding drugs were intravenously injected with dose of 5 mg oxaliplatin per kg of mouse body weight. After 24 h, the mice were executed and the organs were collected. To characterize the distribution in tumor tissue, twelve HCT116 xenograft mice were divided into four groups including oxaliplatin/poly-CB[7] group, oxaliplatin/CB[7] group and oxaliplatin group. Each group contained 4 mice. The corresponding drugs were intravenously injected with dose of 5

mg oxaliplatin per kg of mouse body weight. After 24 h, the mice were executed and the tumors were collected. The samples were digested with HNO_3 and $HClO_4$, and the content of platinum was determined by employing ICP-MS.

3. Results and discussion

3.1. Poly-CB[7] and its host-guest interaction with oxaliplatin

To realize supramolecular polymeric chemotherapy, poly-CB[7] needs to be synthesized which bear CB[7] motif for supramolecular chemotherapy and PEG motif for enhancing circulation performance. In order to introduce CB[7] into the polymers, functionalization of CB[7] becomes inevitable. Hydroxyl group was firstly introduced on the periphery of CB[7] through oxidation of CB[7] with persulfate [45,47]. Further etherification of bis-hydroxyl CB[7] with propargyl bromide yielded bis-alkynyl CB[7] [46], which was then polymerized with α,ω-diazide polyethylene glycol through click reaction to form the desired poly-CB[7] (see supplementary data). The number-average molecular weight of poly-CB[7] was determined to be 6.4×10^4 g/mol by employing GPC-MALLS, namely there are 19 CB[7] units in one polymer chain in average.

We wondered if poly-CB[7] could be used to complex with oxaliplatin. NMR and ITC were employed to characterize the host-guest interaction between poly-CB[7] and oxaliplatin. As shown in Fig. 1a, the proton signals ascribed to oxaliplatin demonstrated up-field shift when mixing oxaliplatin with poly-CB[7], indicating that oxaliplatin was encapsulated in the cavity of CB[7] moiety of poly-CB[7]. ITC was used to further support the host-guest interaction between poly-CB[7] and oxaliplatin. As shown in Fig. 1b, there was an abrupt transition which appeared at the molar ratio of 1:1, indicating that oxaliplatin was complexed with CB[7] of poly-CB[7] in 1:1 binding mode. The titration curve was also fitted with one set of sites model, and the binding constant between oxaliplatin and CB[7] moiety was determined to be 1.8×10^6 M^{-1}. Based on the strong specific binding of oxaliplatin to poly-CB[7], the encapsulation efficiency was approximately 99% under the administration condition, and the loading efficiency of oxaliplatin by poly-CB[7] was 12.1 w/w%. The high binding constant would also helpful in preventing premature release of oxaliplatin. For example, the concentration of oxaliplatin and CB[7] unit in blood was roughly 100 μM within

the dose of 5 mg oxaliplatin per kg of mouse body weight, suggesting that over 90% oxaliplatin stayed bounded in blood with an idealized estimation.

3.2. Decreased cytotoxicity to colorectal normal cells and increased cytotoxicity to colorectal cancer cells of oxaliplatin by complexation with poly-CB[7]

Considering that oxaliplatin can be used for colorectal cancer treatment [7], we chose colorectal normal cell (NCM460 cell line) and colorectal cancer cell (HCT116 cell line) to test the cytotoxicity of oxaliplatin *in vitro* before and after host-guest complexation. As shown in Fig. 2a, poly-CB[7] itself demonstrated almost no cytotoxicity under the experimental conditions, which is essential for its application as drug carrier. For oxaliplatin, as expected, it displayed strong cytotoxicity to colorectal normal cell. Under the condition of 100 μM oxaliplatin, about 81% cells were killed. Interestingly, after complexation with poly-CB[7], the cytotoxicity of oxaliplatin decreased significantly. Under the same condition, only about 8% cells were killed. Further increase in incubation time of oxaliplatin/poly-CB[7] complex led to decrease in cell viability (see Fig. 2b). However, even extending the incubation time to 72 h, 72% cells still survived. These results indicate that poly-CB[7] can effectively decrease the cytotoxicity of oxaliplatin to normal cells, which may be helpful in increasing the safety and decreasing the side-effects of oxaliplatin.

In case of colorectal cancer cell, as shown in Fig. 2c, poly-CB[7] itself demonstrated negligible anticancer activity. As expected, oxaliplatin could kill the cancer cells. With 100 μM oxaliplatin, 75% cancer cells were killed. We found interestingly that oxaliplatin/poly-CB[7] complex demonstrated even higher cytotoxicity to cancer cells than oxaliplatin itself. Under the same condition, 85% cancer cells were killed. It is known that colorectal cancer cell can overexpress spermine [34,35]. Spermine might competitively replace oxaliplatin from the host-guest complex of oxaliplatin/poly-CB[7], and the cytotoxicity of oxaliplatin recovered. In addition, as spermine benefits to cell growth and proliferation [48], the consumption of spermine during competitive release of oxaliplatin may also help in increasing the anticancer activity of oxaliplatin. Increase in incubation time of oxaliplatin/poly-CB[7] complex led to further killing of HCT116 cells (see Fig. 2d). When incubation time increased to 72 h, 96% cancer cells were killed. Therefore, the increased anticancer activity of oxaliplatin/poly-CB[7] is rationalized by the selective release of

oxaliplatin from the host-guest complex and consumption of the spermine in the micro-environment of cancer cells.

3.3. Competitive replacement of oxaliplatin from oxaliplatin/poly-CB[7] complex by spermine

To elucidate the mechanism behind the competitive replacement of oxaliplatin by spermine, *in vitro* experiments were performed. The binding of spermine to poly-CB[7] was firstly characterized by employing ^{1}H NMR and ITC. As shown in Fig. 3a, after mixing spermine with poly-CB[7], the proton signals ascribed to butylene moiety of spermine exhibited up-field shift and the proton signals ascribed to propylene moiety demonstrated down-field shift, indicating that butylene moiety of spermine was encapsulated in the CB[7] cavity of poly-CB[7]. Through ITC experiment (Fig. 3b), spermine also displayed 1:1 binding mode with CB[7] moiety of poly-CB[7]. The binding constant between poly-CB[7] and spermine was determined to be 4.9×10^{5} M^{-1} in phosphate buffer solution with pH of 6.0. Considering the similar binding affinity of oxaliplatin and spermine to poly-CB[7], the release proportion of oxaliplatin is determined by the concentration of spermine.

UV-vis titration was employed to monitor the competitive replacement of oxaliplatin from its complex with poly-CB[7]. The host-guest complexation of poly-CB[7] and oxaliplatin led to increase in absorbance of oxaliplatin in the range of 245-280 nm. And dissociation of the host-guest complex resulted in the decrease of absorbance to original level. Through titrating spermine into the solution of oxaliplatin/poly-CB[7] complex, decrease in absorbance was observed, suggesting the dissociation of oxaliplatin from the oxaliplatin/poly-CB[7] complex (see supplementary data). We then selected the absorbance at 258 nm to calculate the release ratio of oxaliplatin. As shown in Fig. 4, 6 equivalent spermine led to the release of around 50% oxaliplatin, and 35 equivalent spermine led to the release of around 90% oxaliplatin from oxaliplatin/poly-CB[7]. The released amount of oxaliplatin was also calculated based on the binding constants of spermine and oxaliplatin to poly-CB[7]. The calculated and measured curves fit well with each other, which further support the experimental results. Thus the competitive replacement of oxaliplatin is concentration dependent. In other words, more oxaliplatin can be released from the host-guest complex with increasing concentration of spermine.

3.4. Increased circulation performance of oxaliplatin by complexation with poly-CB[7]

Poly-CB[7] was expected to prolong the circulation performance of oxaliplatin in blood based on the PEG structure. To verify this assumption, *in vivo* experiments were performed through the intravenous injection of oxaliplatin and oxaliplatin/poly-CB[7] complex on KM mice. The blood platinum concentrations at varied time were tested by employing ICP-MS. As shown in Fig. 5, the mice that intravenously administrated with oxaliplatin/poly-CB[7] complex demonstrated significantly higher blood platinum concentration than the oxaliplatin group. The area under the curve (AUC) in blood of oxaliplatin/poly-CB[7] group was 60.5 μg/mL·h, which was 21.6-fold higher than oxaliplatin group. To exclude the possible enhancement of CB[7] moiety to circulation performance of oxaliplatin, oxaliplatin/CB[7] group was also included in Fig. 5. Oxaliplatin/CB[7] group exhibited AUC value of 1.29 μg/mL·h, which is similar to the level of oxaliplatin group rather than oxaliplatin/poly-CB[7] group. Therefore poly-CB[7] can sufficiently enhance the circulation performance of oxaliplatin because of the PEG structure of poly-CB[7].

3.5. *In vivo* antitumor bioactivity and side-effect evaluation of oxaliplatin before and after complexation with poly-CB[7]

We assessed the xenograft tumor growth of HCT116 tumor with intravenous administration of oxaliplatin, oxaliplatin/poly-CB[7] and oxaliplatin/CB[7] to evaluate their antitumor bioactivity and safety (see Fig. 6). The mice were treated with an equivalent dose of 5 mg oxaliplatin per kg of body weight for six times during two weeks. The tumor volumes were monitored during the therapeutic process. It was demonstrated that oxaliplatin/poly-CB[7] might inhibit the growth of tumor with higher bioactivity than oxaliplatin itself, but the enhancement was limited. The reason may be attributed to that whilst the PEG structure of poly-CB[7] enhanced the circulation performance of oxaliplatin, the PEG structure also hinder the interaction and internalization of oxaliplatin to tumor tissue [49]. The body weight of mice during the therapeutic process was also monitored (Fig. 6b). The relative body weight of oxaliplatin/poly-CB[7] group was similar to the value of control group, indicating that the side-effect of oxaliplatin/poly-CB[7] is acceptable. Compared with the lower relative body weight of oxaliplatin group, it is clearly shown that poly-CB[7] can decrease the side-effect of oxaliplatin. Considering oxaliplatin/CB[7] group displayed similar

relative body weight to oxaliplatin/poly-CB[7] group, the enhancement in safety is probably caused by the host-guest interaction between oxaliplatin and CB[7] moiety, which is in agreement with the results in cell experiments. Therefore, the advantage of oxaliplatin/poly-CB[7] is its enhanced safety compared with oxaliplatin.

3.6. *In vivo* tissue distribution of platinum by the administration of oxaliplatin, oxaliplatin/poly-CB[7] and oxaliplatin/CB[7]

To elucidate the limited improvement on antitumor bioactivity of oxaliplatin through the complexation of poly-CB[7], we studied platinum distribution in tissue after intravenous injection of oxaliplatin, oxaliplatin/poly-CB[7] and oxaliplatin/CB[7]. The mice were treated with an equivalent dose of 5 mg oxaliplatin per kg of body weight. They were executed after 24 h and the organs and tumors were collected and digested for further analyzation. As shown in Fig. 7, host-guest complexation of oxaliplatin by poly-CB[7] significantly changed the distribution of oxaliplatin, whilst the complexation of oxaliplatin by CB[7] demonstrated minor influence on the distribution of oxaliplatin. The complexation of oxaliplatin by poly-CB[7] increased the platinum distribution in liver and spleen, decreased the platinum distribution in heart, lung and kidney, but did not significantly change the platinum distribution in tumors. Considering the fact that the plasma platinum concentration of oxaliplatin/poly-CB[7] group was significantly higher than oxaliplatin group, poly-CB[7] might hinder the interaction and internalization of oxaliplatin to tissue and cells. These results also interpret the question that why the increased circulation performance of oxaliplatin did not translate into better antitumor bioactivity. The increased circulation performance could be offset by the decreased interaction and internalization, and the similar amount of oxaliplatin in tumor leads to similar therapeutic performance.

4. Conclusions

In summary, we have developed a new strategy of supramolecular polymeric chemotherapy to enhance the circulation performance and safety of oxaliplatin by the complexation between poly-CB[7] and oxaliplatin. It works with cancer cells which can overexpress spermine, such as colorectal cancer cells. We expect that more functions such as targeting ability and responsiveness to tumor microenvironment may be also introduced into

the polymeric systems through polymerization, which may help in increasing the accumulation of therapeutic agent in tumor. In addition to oxaliplatin, poly-CB[7] could encapsulate other kind of antitumor drugs for decreasing their cytotoxicity to normal cells and increasing cytotoxicity to cancer cells. With an appropriate choice of anticancer drugs which can complex with poly-CB[7] in a lower binding affinity than spermine, the antitumor drugs may release completely for enhancing the antitumor bioactivity. It is anticipated that this line of research may open new horizons for supramolecular polymeric chemotherapy.

Acknowledgements

This work was supported by the National Natural Science Foundation of China (21434004, 91527000) and Postdoctoral Innovation Talents Support Program (BX201600083).

References

[1] P.M. Kasi, A. Grothey, Chemotherapy maintenance, Cancer J. 22 (2016) 199-204.
[2] M.A. Jordan, K. Wendell, S. Gardiner, W.B. Derry, H. Copp, L. Wilson, Mitotic block induced in HeLa cells by low concentrations of paclitaxel (Taxol) results in abnormal mitotic exit and apoptotic cell death, Cancer Res. 56 (1996) 816-825.
[3] A. Sandler, R. Gray, M.C. Perry, J. Brahmer, J.H. Schiller, A. Dowlati, R. Lilenbaum, D.H. Johnson, Paclitaxel-carboplatin alone or with bevacizumab for non-small-cell lung cancer, N. Engl. J. Med. 355 (2006) 2542-2550.
[4] M.E. Wall, M.C. Wani, Camptothecin and Taxol: Discovery to clinic - Thirteenth Bruce F. Cain Memorial Award Lecture, Cancer Res. 55 (1995) 753-760.
[5] N.H. Oberlies, D.J. Kroll, Camptothecin and Taxol: historic achievements in natural products research, J. Nat. Prod. 67 (2004) 129-135.
[6] A. Gabizon, H. Shmeeda, Y. Barenholz, Pharmacokinetics of pegylated liposomal doxorubicin-Review of animal and human studies, Clin. Pharmacokinet. 42 (2003) 419-436.
[7] L. Kelland, The resurgence of platinum-based cancer chemotherapy, Nat. Rev. Cancer 7 (2007) 573-584.
[8] J.-C. Huang, D.B. Zamble, J.T. Reardon, S.J. Lippard, A. Sancar, HMG-domain proteins specifically inhibit the repair of the major DNA adduct of the anticancer drug cisplatin by human excision nuclease, Proc. Natl. Acad. Sci. USA 91 (1994) 10394-10398.
[9] P.G. Corrie, Cytotoxic chemotherapy: clinical aspects, Medicine 39 (2011) 717-722.
[10] H. Chen, W. Zhang, G. Zhu, J. Xie, X. Chen, Rethinking cancer nanotheranostics, Nat. Rev. Mater. 2 (2017) 17024.
[11] C. Liang, L. Xu, G. Song, Z. Liu, Emerging nanomedicine approaches fighting tumor

metastasis: animal models, metastasis-targeted drug delivery, phototherapy, and immunotherapy, Chem. Soc. Rev. 45 (2016) 6250-6269.

[12] I.H. Park, J.H. Sohn, S.B. Kim, K.S. Lee, J.S. Chung, S.H. Lee, T.Y. Kim, K.H. Jung, E.K. Cho, Y.S. Kim, H.S. Song, J.H. Seo, H.M. Ryoo, S.A. Lee, S.Y. Yoon, C.S. Kim, Y.T. Kim, S.Y. Kim, M.R. Jin, J. Ro, An open-label, randomized, parallel, phase III trial evaluating the efficacy and safety of polymeric micelle-formulated paclitaxel compared to conventional Cremophor EL-based paclitaxel for recurrent or metastatic HER_2-negative breast cancer, Cancer Res. Treat. 49 (2017) 569-577.

[13] X. Luan, Y.-Y. Guan, J.F. Lovell, M. Zhao, Q. Lu, Y.-R. Liu, H.-J. Liu, Y.-G. Gao, X. Dong, S.-C. Yang, L. Zheng, P. Sun, C. Fang, H.-Z. Chen, Tumor priming using metronomic chemotherapy with neovasculature-targeted, nanoparticulate paclitaxel, Biomaterials 95 (2016) 60-73.

[14] K.H. Min, K. Park, Y.-S. Kim, S.M. Bae, S. Lee, H.G. Jo, R.-W. Park, I.-S. Kim, S.Y. Jeong, K. Kim, I.C. Kwon, Hydrophobically modified glycol chitosan nanoparticles-encapsulated camptothecin enhance the drug stability and tumor targeting in cancer therapy, J. Control. Release 127 (2008) 208-218.

[15] G.H. Petersen, S.K. Alzghari, W. Chee, S.S. Sankari, N.M. La-Beck, Meta-analysis of clinical and preclinical studies comparing the anticancer efficacy of liposomal versus conventional non-liposomal doxorubicin, J. Control. Release 232 (2016) 255-264.

[16] C. Wang, L.A. Cheng, Z.A. Liu, Drug delivery with upconversion nanoparticles for multi-functional targeted cancer cell imaging and therapy, Biomaterials 32 (2011) 1110-1120.

[17] J. Chen, J. Ding, Y. Wang, J. Cheng, S. Ji, X. Zhuang, X. Chen, Sequentially responsive shell-stacked nanoparticles for deep penetration into solid tumors, Adv. Mater. 29 (2017) 1701170.

[18] J. Chen, J. Ding, W. Xu, T. Sun, H. Xiao, X. Zhuang, X. Chen, Receptor and microenvironment dual-recognizable nanogel for targeted chemotherapy of highly metastatic malignancy, Nano Lett. 17 (2017) 4526-4533.

[19] Q. Chen, H.T. Ke, Z.F. Dai, Z. Liu, Nanoscale theranostics for physical stimulus-responsive cancer therapies, Biomaterials 73 (2015) 214-230.

[20] S.-Y. Qin, A.-Q. Zhang, S.-X. Cheng, L. Rong, X.-Z. Zhang, Drug self-delivery systems for cancer therapy, Biomaterials 112 (2017) 234-247.

[21] F. Li, T. Li, W. Cao, L. Wang, H. Xu, Near-infrared light stimuli-responsive synergistic therapy nanoplatforms based on the coordination of tellurium-containing block polymer and cisplatin for cancer treatment, Biomaterials 133 (2017) 208-218.

[22] P. Cai, W.R. Leow, X. Wang, Y.-L. Wu, X. Chen, Programmable nano-bio interfaces for functional biointegrated devices, Adv. Mater. 29 (2017) 1605529.

[23] T. Li, W. Xiang, F. Li, H. Xu, Self-assembly regulated anticancer activity of platinum coordinated selenomethionine, Biomaterials 157 (2018) 17-25.

[24] Y.-L. Wu, W. Engl, B. Hu, P. Cai, W.R. Leow, N.S. Tan, C.T. Lim, X. Chen, Nanomechanically visualizing drug-cell interaction at the early stage of chemotherapy, ACS Nano 11 (2017) 6996-7005.

[25] O. Lyass, B. Uziely, R. Ben-Yosef, D. Tzemach, N.I. Heshing, M. Lotem, G. Brufman, A. Gabizon, Correlation of toxicity with pharmacokinetics of pegylated liposomal doxorubicin (Doxil) in metastatic breast carcinoma, Cancer 89 (2000) 1037-1047.

[26] J.L. Villano, D. Mehta, L. Radhakrishnan, Abraxane® induced life-threatening toxicities with metastatic breast cancer and hepatic insufficiency, Invest. New Drug 24 (2006) 455-456.
[27] K.S. Lee, H.C. Chung, S.A. Im, Y.H. Park, C.S. Kim, S.-B. Kim, S.Y. Rha, M.Y. Lee, J. Ro, Multicenter phase II trial of Genexol-PM, a Cremophor-free, polymeric micelle formulation of paclitaxel, in patients with metastatic breast cancer, Breast Cancer Res. Treat. 108 (2008) 241-250.
[28] N. Saleh, A.L. Koner, W.M. Nau, Activation and stabilization of drugs by supramolecular pK_a shifts: drug-delivery applications tailored for cucurbiturils, Angew. Chem. Int. Ed. 47 (2008) 5398-5401.
[29] N.J. Wheate, A.I. Day, R.J. Blanch, A.P. Arnold, C. Cullinane, J.G. Collins, Multi-nuclear platinum complexes encapsulated in cucurbit[n]uril as an approach to reduce toxicity in cancer treatment, Chem. Commun. (2004) 1424-1425.
[30] H. Yang, C. Song, H. Chen, W. Xu, Y. Tan, Synthesis, characterisation and properties of star polypseudorotaxanes with cucurbit[7]uril, Supramol. Chem. 24 (2012) 833-840.
[31] Y. Chen, Z. Huang, J.-F. Xu, Z. Sun, X. Zhang, Cytotoxicity regulated by host-guest interactions: A supramolecular strategy to realize controlled disguise and exposure, ACS Appl. Mater. Interfaces 8 (2016) 22780-22784.
[32] Y. Chen, Z. Huang, H. Zhao, J.-F. Xu, Z. Sun, X. Zhang, Supramolecular chemotherapy: Cooperative enhancement of antitumor activity by combining controlled release of oxaliplatin and consuming of spermine by cucurbit[7]uril, ACS Appl. Mater. Interfaces 9 (2017) 8602-8608.
[33] Q. Hao, Y. Chen, Z. Huang, J.-F. Xu, Z. Sun, X. Zhang, Supramolecular chemotherapy: Carboxylated pillar[6]arene for decreasing cytotoxicity of oxaliplatin to normal cells and improving its anticancer bioactivity against colorectal cancer, ACS Appl. Mater. Interfaces (2018) DOI: 10.1021/acsami.7b19784.
[34] D.H. Russell, Clinical relevance of polyamines as biochemical markers of tumor kinetics, Clin. Chem. 23 (1977) 22-27.
[35] A.N. Kingsnorth, A.B. Lumsden, H.M. Wallace, Polyamines in colorectal cancer, Brit. J. Surg. 71 (1984) 791-794.
[36] H. Ringsdorf, Structure and properties of pharmacologically active polymers, J. Polym. Sci. Polym. Symp. 51 (1975) 135-153.
[37] L. Gros, H. Ringsdorf, H. Schupp, Polymeric antitumor agents on a molecular and on a cellular level, Angew. Chem. Int. Ed. 20 (1981) 305-325.
[38] R. Haag, F. Kratz, Polymer therapeutics: Concepts and applications, Angew. Chem. Int. Ed. 45 (2006) 1198-1215.
[39] K. Knop, R. Hoogenboom, D. Fischer, U.S. Schubert, Poly(ethylene glycol) in drug delivery: Pros and cons as well as potential alternatives, Angew. Chem. Int. Ed. 49 (2010) 6288-6308.
[40] A. Kolate, D. Baradia, S. Patil, I. Vhora, G. Kore, A. Misra, PEG - A versatile conjugating ligand for drugs and drug delivery systems, J. Control. Release 192 (2014) 67-81.
[41] A. Day, A.P. Arnold, R.J. Blanch, B. Snushall, Controlling factors in the synthesis of cucurbituril and its homologues, J. Org. Chem. 66 (2001) 8094-8100.
[42] J. Kim, I.-S. Jung, S.-Y. Kim, E. Lee, J.-K. Kang, S. Sakamoto, K. Yamaguchi, K. Kim, New cucurbituril homologues: Syntheses, isolation, characterization, and X-ray crystal

structures of cucurbit[n]uril (n = 5, 7, and 8), J. Am. Chem. Soc. 122 (2000) 540-541.
[43] H. Chen, S. Hou, Y. Tan, An 'in-water' halogen-ion compatible "click" catalyst for cucurbituril guest ligation, Supramol. Chem. 28 (2016) 801-809.
[44] N. Zhao, G.O. Lloyd, O.A. Scherman, Monofunctionalised cucurbit[6]uril synthesis using imidazolium host-guest complexation, Chem. Commun. 48 (2012) 3070-3072.
[45] H. Chen, H. Ma, Y. Tan, Synthesis of linear cucurbit[7]uril pendent copolymers through radical polymerization: Polymers with ultra-high binding affinity, J. Polym. Sci. Polym. Chem. 53 (2015) 1748-1752.
[46] H. Chen, Z. Huang, H. Wu, J.-F. Xu, X. Zhang, Supramolecular polymerization controlled through kinetic trapping, Angew. Chem. Int. Ed. 56 (2017) 16575-16578.
[47] S.Y. Jon, N. Selvapalam, D.H. Oh, J.-K. Kang, S.-Y. Kim, Y.J. Jeon, J.W. Lee, K. Kim, Facile synthesis of cucurbit[n]uril derivatives via direct functionalization: expanding utilization of cucurbit[n]uril, J. Am. Chem. Soc. 125 (2003) 10186-10187.
[48] X. Wang, Y. Ikeguchi, D.E. McCloskey, P. Nelson, A.E. Pegg, Spermine synthesis is required for normal viability, growth, and fertility in the mouse, J. Biol. Chem. 279 (2004) 51370-51375.
[49] Q. Sun, Z. Zhou, N. Qiu, Y. Shen, Rational design of cancer nanomedicine: Nanoproperty integration and synchronization, Adv. Mater. 29 (2017) 1606628.

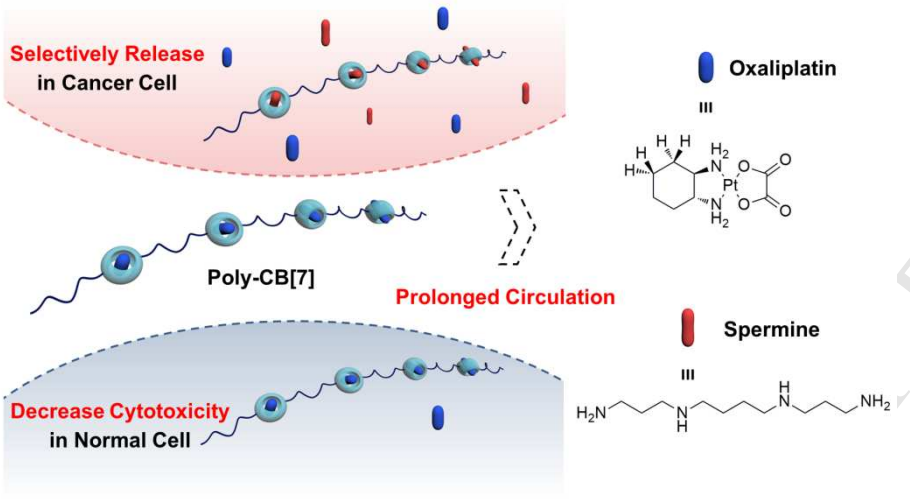

Scheme 1. Schematic illustration of supramolecular polymeric chemotherapy based on poly-CB[7]. Poly-CB[7] can enhance the circulation performance of oxaliplatin and realize selectively release of oxaliplatin in cancer cells which can overexpress spermine.

1.5-column fitting image for **Scheme 1**.

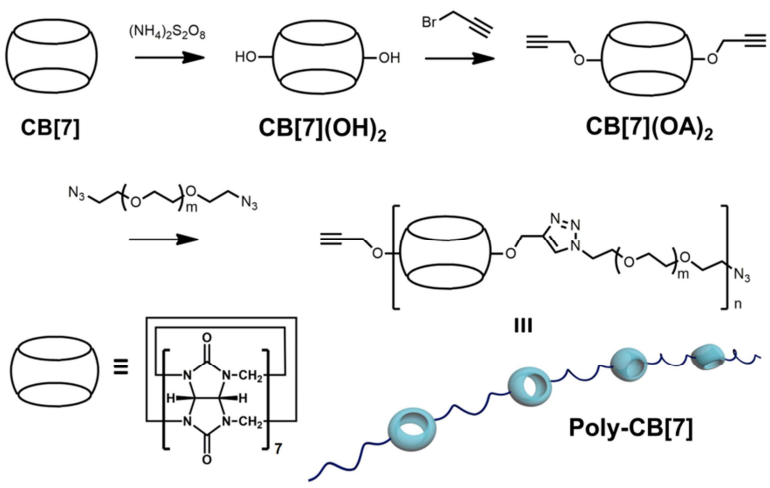

Scheme 2. Schematic illustration of the synthesis procedure of poly-CB[7].

1.5-column fitting image for **Scheme 2**.

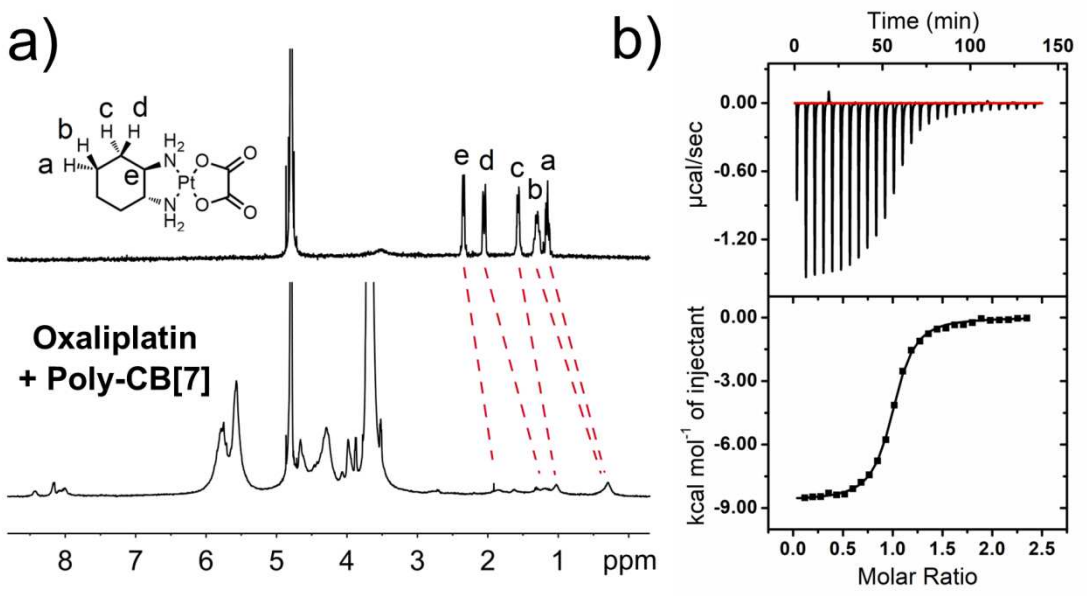

Fig. 1. Host-guest interaction between poly-CB[7] and oxaliplatin characterized by employing a) ^{1}H NMR and b) ITC in 20 mM phosphate buffer solution at pH 6.0.

1.5-column fitting image for **Fig. 1**.

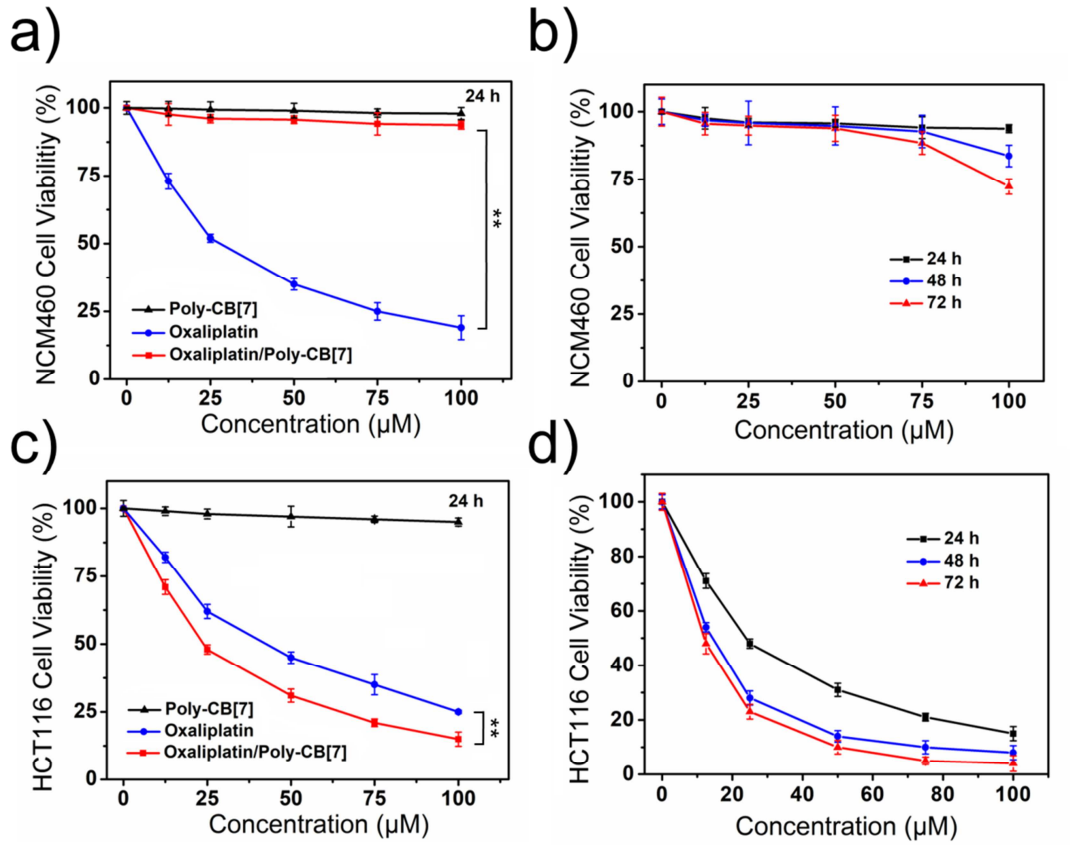

Fig. 2. *In vitro* cytotoxicity of a) poly-CB[7], oxaliplatin and oxaliplatin/poly-CB[7] complex to NCM460 cell line incubated for 24 h, b) oxaliplatin/poly-CB[7] complex to NCM460 cell

line incubated for varied time, c) poly-CB[7], oxaliplatin and oxaliplatin/poly-CB[7] complex to HCT116 cell incubated for 24 h and d) oxaliplatin/poly-CB[7] complex to HCT116 cell incubated for varied time. The concentration is given with equivalent dose of oxaliplatin. Data are presented as mean ± SD with n = 5. **p < 0.01 for comparing oxaliplatin/poly-CB[7] group with oxaliplatin group by employing one-way ANOVA.

1.5-column fitting image for **Fig. 2**.

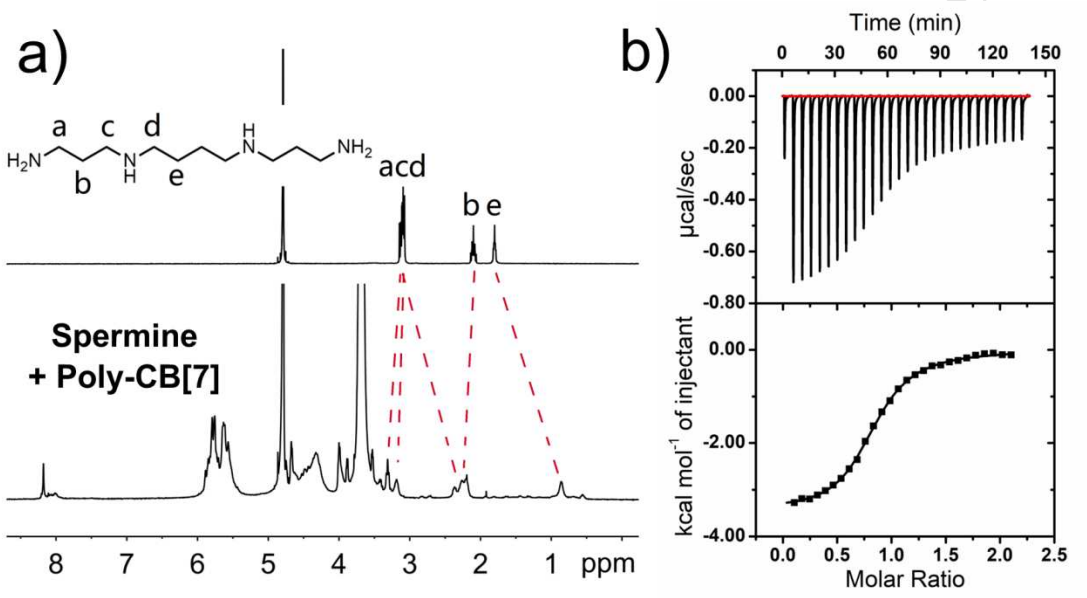

Fig. 3. Host-guest interaction between poly-CB[7] and spermine characterized by employing a) ^{1}HNMR and b) ITC in 20 mM phosphate buffer solution at pH 6.0.

1.5-column fitting image for **Fig. 3**.

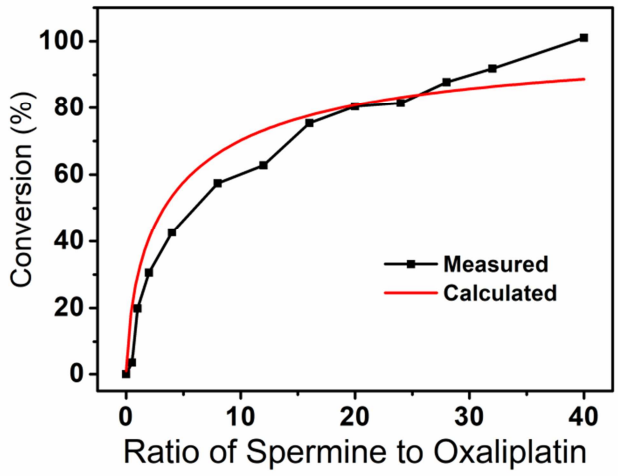

Fig. 4. Competitive replacement of oxaliplatin from oxaliplatin/poly-CB[7] complex with varied ratio of spermine measured by employing UV titration and calculated based on the binding constants of spermine and oxaliplatin to poly-CB[7].

single-column fitting image for **Fig. 4**.

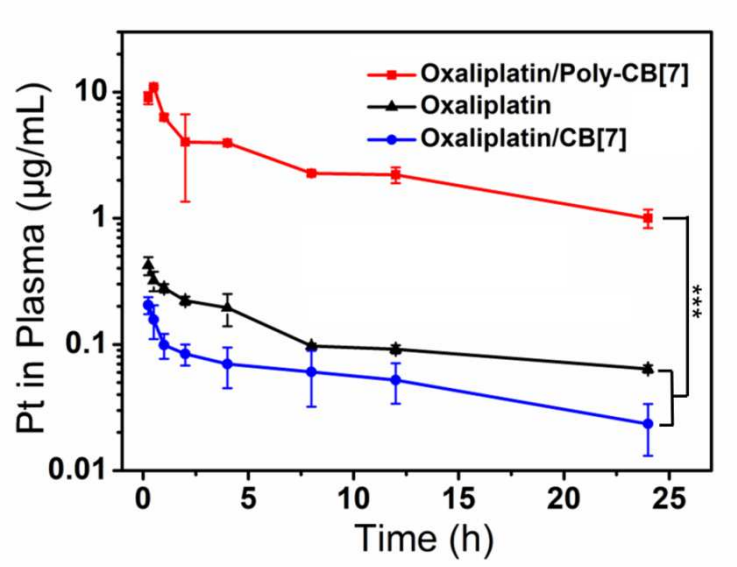

Fig. 5. Plasma platinum concentration versus time after intravenous injection of oxaliplatin, oxaliplatin/poly-CB[7] and oxaliplatin/CB[7]. Data are presented as mean ± SD with n = 3. ***$p < 0.001$ by employing one-way ANOVA.

single-column fitting image for **Fig. 5**.

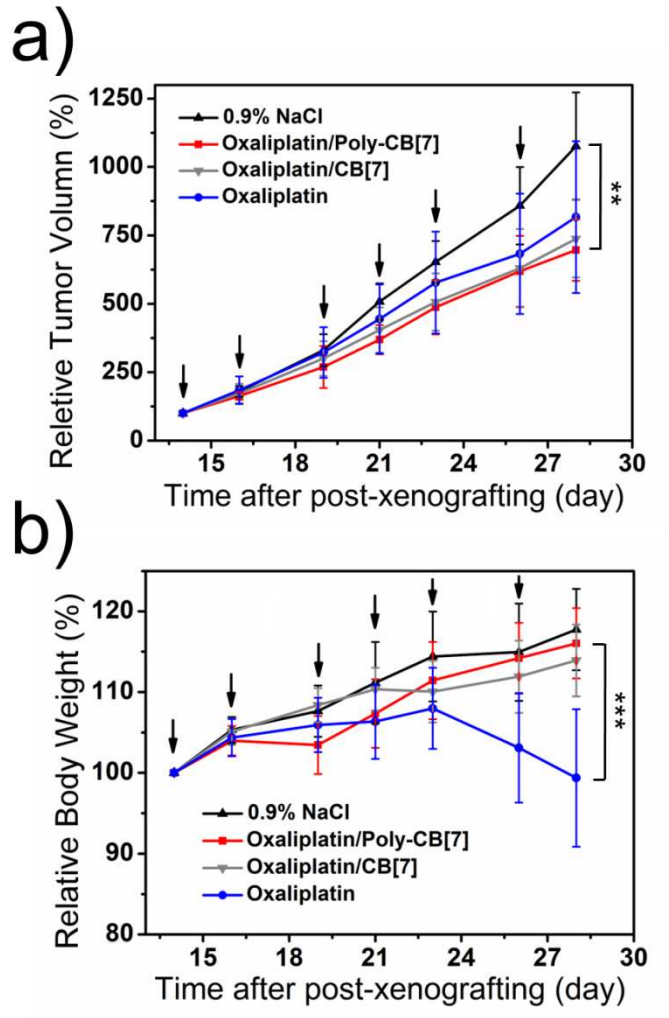

Fig. 6. a) Inhibition of tumor growth and b) relative body weight of BALB/c nude mice with HCT116 xenografts after six treatment with oxaliplatin, oxaliplatin/poly-CB[7] and oxaliplatin/CB[7]. Data are presented as mean ± SD with n = 10. **p < 0.01 and ***p < 0.001 for comparing oxaliplatin/poly-CB[7] group with control group and oxaliplatin/poly-CB[7] group with oxaliplatin group at day 28 by employing one-way ANOVA.

single-column fitting image for **Fig. 6**.

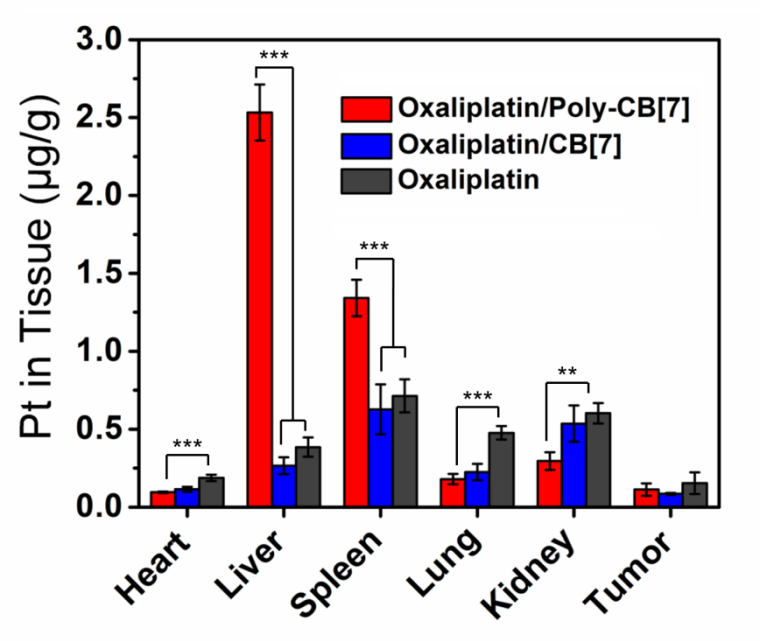

Fig. 7. Tissue distribution of platinum upon the *in vivo* administration of oxaliplatin, oxaliplatin/poly-CB[7] and oxaliplatin/CB[7]. Data are presented as mean ± SD with n = 4. **p < 0.01 and ***p < 0.001 for comparing oxaliplatin/poly-CB[7] group with oxaliplatin and oxaliplatin/CB[7] groups by employing one-way ANOVA.

single-column fitting image for **Fig. 7**.